

# Frequency-Domain Measurement of the Spin Imbalance Lifetime in Superconductors

C. H. L. Quay,<sup>1,\*</sup> C. Dutreix,<sup>1</sup> D. Chevallier,<sup>2</sup> C. Bena,<sup>1,3</sup> and M. Aprili<sup>1</sup>

<sup>1</sup>*Laboratoire de Physique des Solides (CNRS UMR 8502),  
Bâtiment 510, Université Paris-Sud, 91405 Orsay, France*

<sup>2</sup>*Instituut-Lorentz, Universiteit Leiden,  
P.O. Box 9506, 2300 RA Leiden, The Netherlands*

<sup>3</sup>*Institut de Physique Théorique, CEA Saclay 91190 Gif-sur-Yvette, France.*

(Dated: December 6, 2024)

## Abstract

We have measured the lifetime of spin imbalances in the quasiparticle population of a superconductor in the frequency domain. A time-dependent spin imbalance is created by injecting spin-polarised electrons into a thin-film mesoscopic superconductor (Al) at finite excitation frequencies and finite magnetic field. The time-averaged value of the spin imbalance as a function of excitation frequency shows a cut-off corresponding to the spin lifetime. The spin lifetime is relatively constant in the accessible ranges of magnetic fields and temperatures; its value is in agreement with previous estimates. Our data are qualitatively well-described by a theoretical model taking into account all quasiparticle tunnelling processes from a normal metal into a superconductor.

PACS numbers: 74.40.Gh, 75.76.+j, 74.78.Na

---

\*Electronic address: charis.quay@u-psud.fr

Spin-polarised electrons injected into superconductors eventually disappear into the condensate, which is made up of Cooper pairs of electrons of opposite spin. To disappear, the injected electrons — which become quasiparticles in the superconductor — must lose energy, flip their spin and recombine with quasiparticles of the opposite spin to form Cooper pairs. These processes may be sequential or occur in parallel. For example, (1) quasiparticles may undergo elastic or inelastic spin flip processes, (2) quasiparticles may lose energy without flipping their spin, and (3) low-energy quasiparticles recombining in pairs necessarily lose a quantity of energy equivalent to the superconducting gap, usually in the form of a phonon. The characteristic timescale for these processes — as well as the order in which they occur and any interdependence between them — can shed light on microscopic properties of the superconductor, including relaxation pathways [1–8] as well as the gap structure and the pairing mechanism in unconventional superconductors [9–12].

Time- and frequency-domain experiments, whether using transport, optical pump-probe or other techniques, provide the most direct measure of the timescales involved [13–16]. Most of the work in this area has focused on the recombination of quasiparticles, usually with techniques sensitive to the number of quasiparticles and their diminution over time. A quasiparticle population which is larger than that at equilibrium does not however exhaust the possible non-equilibrium phenomena: the quasiparticle population can also manifest spin and/or charge imbalances [17–23]. These do not necessarily relax in the same way, nor on the same timescale. In this Letter we report the first frequency-domain measurement of the lifetime of a spin imbalance in the quasiparticle population in a mesoscopic superconductor.

The idea of our experiment, in brief, is as follows: We inject spin-polarised quasiparticles into a superconductor at a finite frequency  $f_{RF} = \omega/2\pi$  while measuring the time-averaged spin-up quasiparticle chemical potential,  $\langle \mu_s(\omega, t) \rangle_t$ . We expect a cut-off at roughly  $\omega = 1/\tau_s$ , with  $\tau_s$  the spin lifetime of quasiparticles in the superconductor (Figure 1b). This is akin to filling a leaky bath from a tap, turned on and off at a regular rhythm, while measuring the time-averaged water level in the bath.

Our samples, fabricated with standard electron-beam lithography and evaporation techniques, are thin-film superconducting (S) bars, with a native insulating (I) oxide layer, across which lie normal metal (N) and ferromagnetic (F) electrodes used either as ‘injectors’ or as ‘detectors’. (Figure 1) In our devices, S is aluminium, I  $\text{Al}_2\text{O}_3$ , F cobalt and N thick aluminium with a critical magnetic field of  $\sim 50\text{mT}$ . (In all the data shown here, this Al electrode

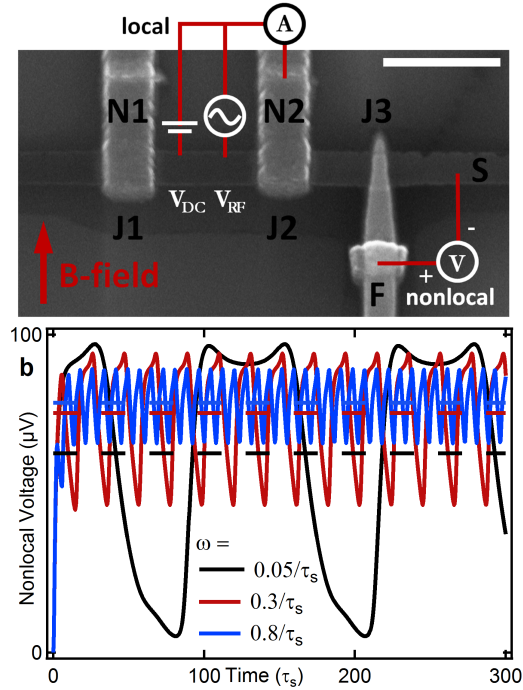


FIG. 1: (a) Scanning electron micrograph of a typical device (scale bar =  $1\mu\text{m}$ ) and schematic drawing of the measurement setup. S = superconductor ( $\sim 8.5\text{nm}$  thick Al film with a native oxide), N = normal metal (100nm Al), F = ferromagnet (40nm Co, with a 4.5nm Al capping layer). The native oxide on S constitutes a tunnel barrier between it and any other given electrode. Quasiparticles are injected into S across a tunnel barrier by applying a voltage  $V_{DC}$  across J1 or J2. These are spin-polarised because of the Zeeman field in S. The nonlocal voltage  $V_{NL}$  and differential nonlocal signal  $dV_{NL}/dV_{DC}$  are measured between a distant ferromagnetic electrode and the superconductor (at J3) as a function of magnetic field and temperature, as well as as a function of the amplitude  $V_{RF}$  and frequency  $f_{RF} = \omega/2\pi$  of high-frequency (1-50MHz) voltages applied to the injection electrode. The local conductance  $dI/dV_{DC}$  is measured simultaneously at the injection electrode. (b) Numerical calculations of  $V_{NL}(t)$  (and its time average) for different  $\omega$ . The time-averaged  $V_{NL}$  depends on  $\omega$ ; this is our main experimental result. These calculation were done for  $V_{DC} = 200\mu\text{V}$ ,  $V_{RF} = 250\mu\text{V}$  and using the measured local conductance at J2 and J3 at 680mT.

is in the normal state.) A typical device is shown in Figure 1a. As in previous experiments, the SIF and NIS junctions have ‘sheet resistances’ respectively of  $\sim 2$  and  $\sim 6 \cdot 10^{-6}\Omega \cdot \text{cm}^2$  (corresponding to barrier transparencies of  $\sim 4$  and  $\sim 1 \cdot 10^{-5}$ ) and tunnelling is the main

transport mechanism across the insulator. (See Supp. Info. of Ref. [19]) Measurements were performed at temperatures down to 50mK, in a dilution refrigerator.

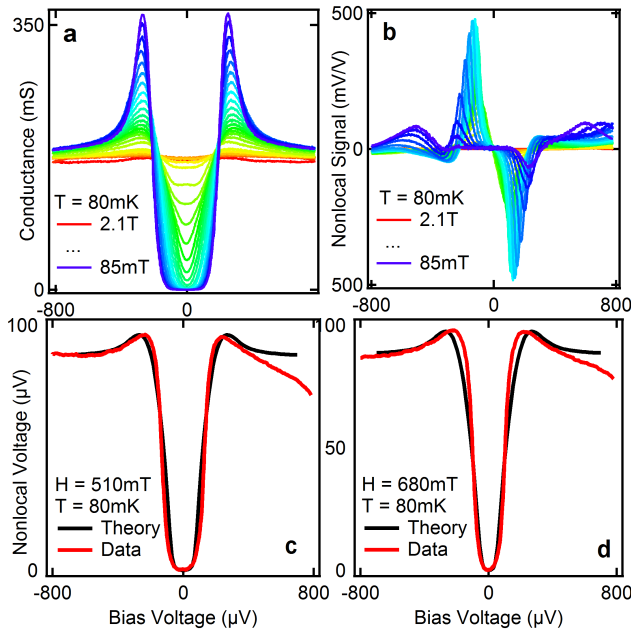


FIG. 2: (a) The conductance  $dI/dV_{DC}$  across J2, which is proportional to the quasiparticle density of states in the superconductor, as a function of  $V_{DC}$  at different magnetic fields. (b) The *differential* nonlocal signal  $dV_{NL}/dV_{DC}$  measured at J3 as a function of  $V_{DC}$  at the same fields. (c,d) Theoretical fits to  $V_{NL}(V_{DC})$  measured at J3 at two different fields. These yield  $\tau_s$  of several nanoseconds.

We simultaneously perform local and non-local transport measurements using standard lock-in techniques: We apply a voltage  $V_{DC}$  across junction J2, between N and S, and measure the (‘local’) current  $I$  injected into the superconductor through J2 and the (‘non-local’) voltages across the other junctions, which act as detectors. We also measure the local conductance  $dI/dV_{DC}$  and the nonlocal differential signal,  $dV_{NL}/dV_{DC}$ . The distance between injection and detection junctions is  $\simeq 1\mu\text{m}$ , well within the Al spin relaxation length in the superconducting state [20]. In the presence of an in-plane magnetic field,  $H$  (applied parallel to the non-superconducting electrodes), electrons injected into the superconductor create a spin imbalance in its quasiparticle population due to the Zeeman effect [19]. The non-local voltage drop  $V_{NL}$  at J3 is proportional to either  $(\mu_{QP\uparrow} - \mu_P)$  or  $(\mu_{QP\downarrow} - \mu_P)$ , depending on the relative alignments of the F magnetisation and the magnetic field. Here  $\mu_{QP\alpha}$  is the chemical potential of the spin  $\alpha$  quasiparticle population and  $\mu_P$  the Cooper

pair chemical potential. We remind the reader that  $\mu_C = (\mu_{QP\uparrow} + \mu_{QP\downarrow})/2$  and  $\mu_S = (\mu_{QP\uparrow} - \mu_{QP\downarrow})/2$  quantify charge and spin accumulation respectively. The non-local voltage drop at J1 is proportional to  $\mu_C - \mu_P$ .

To explore the frequency dependence of the spin imbalance, we add higher-frequency components of amplitude  $V_{RF}$  and frequency  $f_{RF} = 500\text{kHz} - 50\text{MHz}$  to  $V_{DC}$  via a bias-tee located next to the device and at low-temperature.

Before presenting the experimental data, let us sketch out our main theoretical expectations. We assume that the spin accumulation,  $S$  in the superconductor satisfies

$$\frac{dS(t)}{dt} = I_s(t) - \frac{S(t)}{\tau_s}, \quad (1)$$

where  $\tau_s$  is the spin relaxation time in the superconductor and  $I_s$  the spin current.

This equation admits an exact analytical solution:

$$S(t) = e^{-t/\tau_s} \int_0^t dt' I_s(t') e^{t'/\tau_s}. \quad (2)$$

We first consider a spin current of the form  $I_s(t) = I_{DC} + I_{RF}e^{i\omega t}$ , where  $I_{DC}$  and  $I_{RF}$  are constants, we then have

$$S(t) = \tau_s I_{DC} + \frac{\tau_s I_{RF}}{1 + \omega^2 \tau_s^2} e^{i(\omega t + \alpha)} + \text{transient terms} \quad (3)$$

with  $\alpha$  a constant phase. The amplitude of the oscillations in  $S(t)$  (and thus  $\mu_s(t)$  and  $V_{NL}(t)$ , the quantity we measure) are frequency-dependent and show a Lorentzian cut-off behaviour. This could be measured with high-frequency detection techniques.

If, however, the spin current is generated by a sinusoidal voltage, which we assume for the moment to be small, we can write

$$I_s(t) = I_s[V(t)] = I_s[V_{DC} + V_{RF}\cos(\omega t)] = \sum_{n=0}^{\infty} \frac{1}{n!} \left. \frac{\partial^n I_s}{\partial V^n} \right|_{V=V_{DC}} [V_{RF}\cos(\omega t)]^n \quad (4)$$

and insert this into Eq. 4 for  $S(t)$ . If the current-voltage characteristic of the injection junction is nonlinear, a frequency cut-off should also appear in the time-averages of  $S(t)$ ,  $\mu_s(t)$  and  $V_{NL}(t)$ . Numerical work, with no approximations and assuming a non-linear injection junction, shows that this is indeed the case for  $\mu_s(t)$  and  $V_{NL}(t)$  though the cut-off was not observable in  $S(t)$  [24]. In the case of linear injection, a non-linear detection junction will nevertheless yield a frequency cut-off in  $V_{NL}(t)$ . In the case of injection which is already non-linear, detector nonlinearity can further enhance the cut-off behaviour. In

our devices, both injection and detection junctions are non-linear, due to the quasiparticle density of states in the superconductor.

Further details of our theoretical model, which takes into account spin but not charge imbalance, can be found in Ref. [24]. Our model is based on previous work by Zhao and Hershfield [22], which takes into account all quasiparticle tunnelling process at a normal-superconducting junction, extended to include the Zeeman effect induced by the magnetic field. In contrast to the (similar) model presented in our previous work [19], no assumptions were made about the amplitude of the Zeeman energy or  $\mu_S$  (which can be up to half the size of the superconducting gap in these measurements).

Turning now to our measurements, we begin by characterising our device in the absence of high-frequency excitation. Figures 2(a) shows the local conductance as a function of bias voltage and magnetic field. We see that, for this device, the superconducting critical field at J2 is  $\sim 1.9T$ . Figure 2(b) shows the corresponding differential nonlocal signal measured at J3. We remind the reader that, as the injection electrode is normal, the (anti-)symmetric part of this signal comes from the charge (spin) imbalance [19]. In contrast, if the injection electrode were ferromagnetic (and the S DOS highly nonlinear), the ‘spin imbalance peaks’ in the differential nonlocal signal would be of unequal heights [20]. As in our previous work, we see a spin signal which first increases with magnetic field then dies out as the magnetic field approaches its critical value. Theoretical fits to these data at fixed magnetic field such as those shown in Figures 2(c) and (d) allow us to estimate the spin lifetime  $\tau_S$  at several magnetic fields, yielding results on the order of several nanoseconds, consistent with previous measurements.

Note that spin lifetimes estimated from these fits are good only to about an order of magnitude as it is difficult to theoretically account for effects on the superconducting DOS due to stray fields coming from the cobalt electrode. We emphasise, nevertheless, that our theoretical model is able to reproduce all qualitative features of our data. (Figures 2–4, Ref. [24])

We apply a magnetic field of  $H = 680mT$  (to obtain a large non-local signal) and a sinusoidal excitation at 1MHz while sweeping the  $V_{DC}$  and varying the RF power. The results are shown in Figures 3(c)–(f). The main effect of the RF excitation on both the local conductance and the nonlocal signal is the phenomenon known as ‘classical rectification’: As sinusoidal signals spend most time at their extrema, each feature in the original trace is

‘split’ by a distance in bias voltage corresponding to the peak-to-peak amplitude of the RF excitation. These splitting of the BCS coherence peaks in the local conductance (Figure 3(c)) as well as that of the spin imbalance peaks in the nonlocal conductance (Figure 3(d)) are well-reproduced qualitatively by our theory. (Figure 3(a-b)) Figure 3 looks the same for all frequencies, modulo an offset in the RF power due to frequency-dependent attenuation in the RF lines. These measurements can thus be used as a calibration of RF power.

We next study the frequency-dependent response of our system at constant RF amplitude, using the value of the local conductance at zero bias voltage as a calibration of RF amplitude. (The RF amplitude can be more accurately determined from the location of the ‘classically rectified’ peaks and is generally  $\sim 250\mu\text{V}$ .) Figure 4a shows the non-local signal as a function of bias voltage at constant RF amplitude at 1MHz and 50MHz. For both frequencies, ‘classically rectified’ peaks appear at the same location, but their amplitudes are different: At frequencies which are high compared to  $\sim 1/2\pi\tau_S$ , the classically-rectified peaks have smaller amplitudes than they do at low frequencies. (Whether peak amplitudes increase or decrease with frequency depend on the particular parameters of the system. [24]) To track the frequency evolution of the peak amplitude, we measure the nonlocal signal as a function of RF frequency at the bias voltages indicated by the dashed lines (Figures 4(c) and (d)). Fitting Lorentzians to our data yields spin lifetimes of 10ns and 16ns, consistent with previous results. However, our numerical results indicate that such fits can over-estimate  $\tau_S$  by a factor of 2–3 depending on the bias voltage at which the cut-off is measured.

Measurements similar to those shown in Figure 4 were also performed at different fields (at the base temperature of the dilution refrigerator,  $\sim 60\text{mK}$ ) and at different temperatures (at 680mT). These results are shown in Figure 5. No significant change in the cut-off frequency (within measurement error) was observed in the range of accessible temperatures and magnetic fields.

To ascertain that the cut-off was not due to the measurement circuit, we modified the latter slightly, obtaining the same result. We measured similar cut-offs in samples with different detector differential resistances at zero applied voltage (different levels of depairing due to stray fields), thus ruling out detector bandwidth effects. We also checked that the injection of electrons at several times the superconducting gap energy did not significantly affect the quasiparticle temperature, thus also ruling out thermoelectric effects. (See Supplementary Information.)

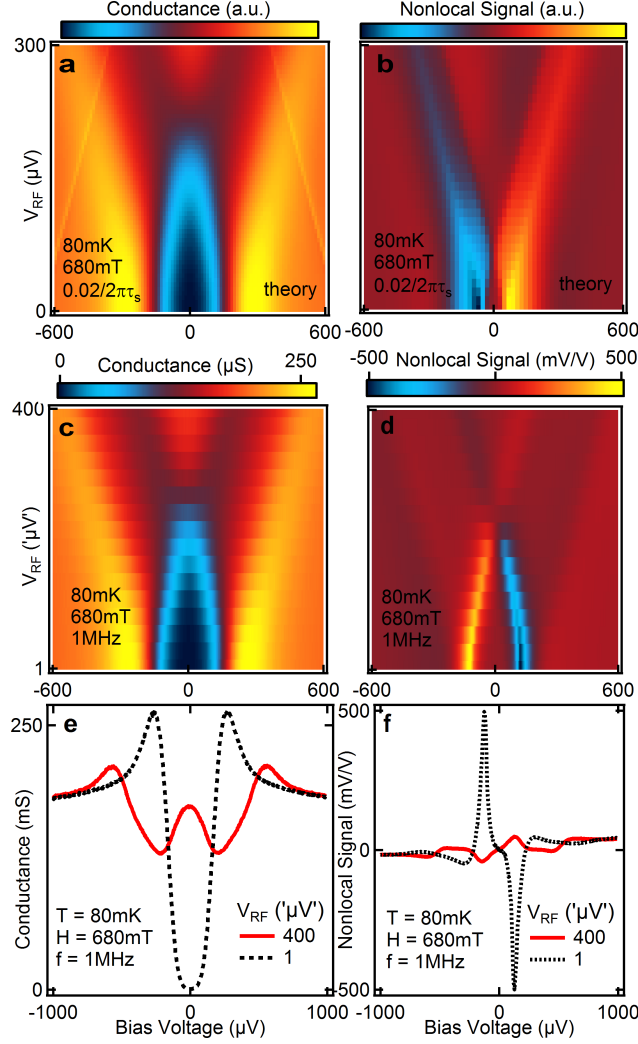


FIG. 3: (a) Calculated local conductance  $dI/dV_{DC}$  as a function of RF amplitude  $V_{RF}$  at a magnetic field of 680mT, based the superconducting DOS extracted from the measured local conductance at  $V_{RF} = 0$ . (b) Calculated differential nonlocal signal  $dV_{NL}/dV_{DC}$  as a function of  $V_{RF}$  at a magnetic field of 680mT, based on the superconducting DOS extracted from the measured local conductance at  $V_{RF} = 0$ . (c) Measured local conductance at J2 as a function of  $V_{RF}$  at  $f_{RF} = 1$ MHz and  $H = 680$ mT. (d) Measured differential nonlocal signal at J3 as a function of of  $V_{RF}$  at  $f_{RF} = 1$ MHz and  $H = 680$ mT. Classical rectification is the dominant RF effect. The  $V_{RF}$  given here are a little higher than what actually arrives at the sample due to attenuation in the line. As noted in the main text,  $V_{RF}$  can in any case be estimated from the classical rectification of features in the  $V_{RF} = 0$  trace. (e,f) Two slices of (c,d).

In conclusion, we have measured the lifetime of spin imbalances in the quasiparticle pop-

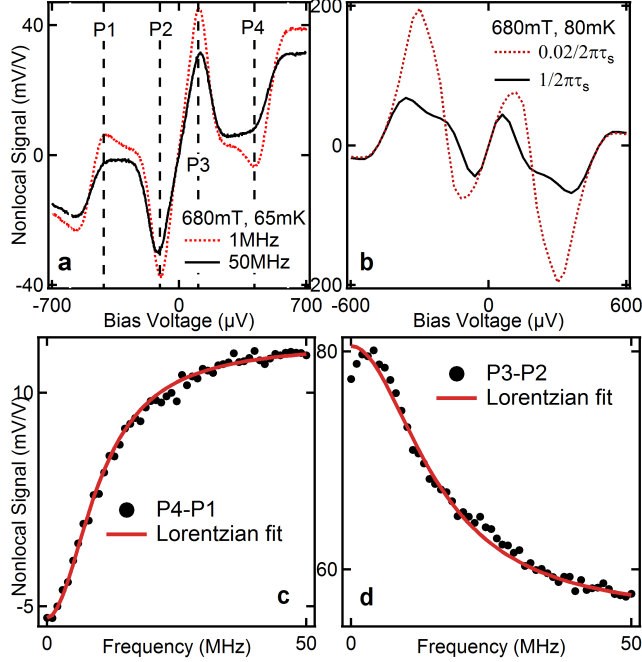


FIG. 4: (a) Measured local conductance  $dI/dV_{DC}$  at J2 as a function of  $V_{DC}$  with constant-power excitations at  $f_{RF} = 1\text{MHz}$ ,  $50\text{MHz}$ . (b) Numerical calculation of the local conductance as a function of  $V_{DC}$  with constant-power excitations at  $f_{RF} = 0.02/2\pi\tau_s$ ,  $1/2\pi\tau_s$ , based on the superconducting DOS extracted from the measured local conductance at  $V_{RF} = 0$ . (c,d) Local conductance at J2 at the  $V_{DC}$  values indicated in (a) as a function of  $f_{RF}$ . We subtract ‘opposing’ peaks to obtain the anti-symmetric part of the signal, which is due to spin. Lorentzian fits give  $\tau_s = 16\text{ns}$  and  $10\text{ns}$  respectively; however, these may be slight over-estimates (see text).

ulation of a superconductor in the frequency domain. This is the most direct measurement to date of this quantity. The charge lifetime could in principle be measured in a similar way, at much higher excitation frequencies. Pushing these experiments one step further, one could look at variations in the spin accumulation either in real-time or at the excitation frequency. All of these techniques could in principle be used to measure spin lifetimes in other superconducting materials.

### Acknowledgments

We thank J. Gabelli for helpful discussions on spin dynamics in superconductors, and J. S. Meyer and M. Houzet for the same on thermoelectric effects. This work was funded by

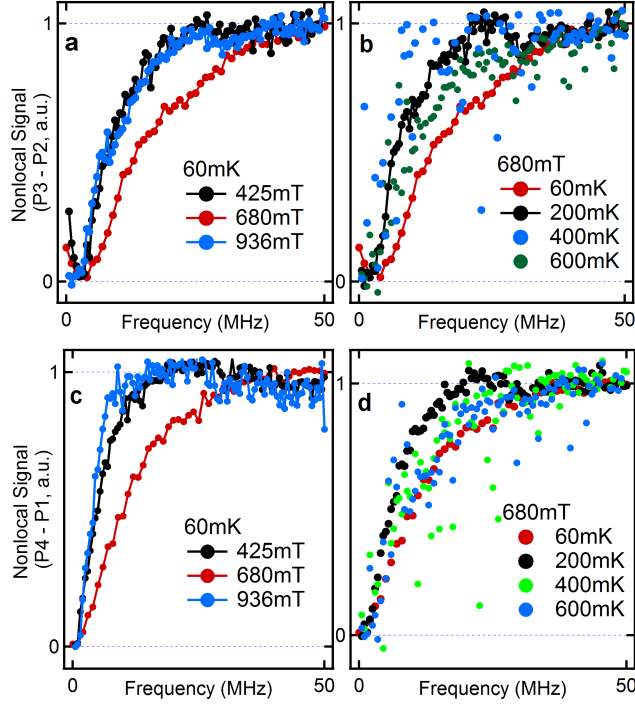


FIG. 5: Local conductance as a function of RF frequency at different fields and temperatures for two different ‘pairs’ of peaks. (cf. Figure 4.). No substantial difference in cut-off frequency is observed in the range of available temperatures and fields.

European Research Council Starting Independent Researcher (NANO-GRAPHENE 256965) and Synergy Grants; an ANR Blanc grant (MASH) from the French Agence Nationale de Recherche; and the Netherlands Organization for Scientific Research (NWO/OCW).

- 
- [1] J. R. Schrieffer and D. M. Ginsberg, *Physical Review Letters* **8**, 207 (1962).
  - [2] A. Rothwarf and B. N. Taylor, *Physical Review Letters* **19**, 27 (1967).
  - [3] C. S. Owen and D. J. Scalapino, *Physical Review Letters* **28**, 1559 (1972).
  - [4] J.-J. Chang and D. J. Scalapino, *Journal of Low Temperature Physics* **31**, 1 (1978).
  - [5] T. P. Devereaux and D. Belitz, *Physical Review B* **44**, 4587 (1991).
  - [6] M. Reizer, *Physical Review B* **61**, 7108 (2000).
  - [7] S. M. Quinlan, D. J. Scalapino, and N. Bulut, *Physical Review B* **49**, 1470 (1994).
  - [8] Y. Yafet, *Physics Letters A* **98**, 287 (1983).
  - [9] R. D. Averitt and A. J. Taylor, *Journal of Physics: Condensed Matter* **14**, R1357 (2002).

- [10] J. Demsar, B. Podobnik, V. V. Kabanov, T. Wolf, and D. Mihailovic, *Physical Review Letters* **82**, 4918 (1999).
- [11] N. Gedik, J. Orenstein, R. Liang, D. A. Bonn, and W. N. Hardy, *Science* **300**, 1410 (2003).
- [12] I. Madan, T. Kurosawa, Y. Toda, M. Oda, T. Mertelj, P. Kusar, and D. Mihailovic, *Scientific Reports* **4** (2014).
- [13] M. Johnson, *Physical Review Letters* **67**, 374 (1991).
- [14] G. L. Carr, R. P. S. M. Lobo, J. LaVeigne, D. H. Reitze, and D. B. Tanner, *Physical Review Letters* **85**, 3001 (2000).
- [15] R. Peters and H. Meissner, *Physical Review Letters* **30**, 965 (1973).
- [16] P. Hu, R. C. Dynes, and V. Narayanamurti, *Physical Review B* **10**, 2786 (1974).
- [17] J. Clarke, *Physical Review Letters* **28**, 1363 (1972).
- [18] M. Tinkham and J. Clarke, *Physical Review Letters* **28**, 1366 (1972).
- [19] C. H. L. Quay, D. Chevallier, C. Bena, and M. Aprili, *Nature Physics* **9**, 84 (2013).
- [20] F. Hübler, M. J. Wolf, D. Beckmann, and H. v. Loehneysen, *Physical Review Letters* **109**, 207001 (2012).
- [21] M. J. Wolf, F. Hübler, S. Kolenda, H. v. Loehneysen, and D. Beckmann, *Physical Review B* **87**, 024517 (2013).
- [22] H. L. Zhao and S. Hershfield, *Physical Review B* **52**, 3632 (1995).
- [23] S. Takahashi, H. Imamura, and S. Maekawa, *Physical Review Letters* **82**, 3911 (1999).
- [24] D. Chevallier, C. Dutreix, M. Guigou, C. H. L. Quay, C. Bena, and M. Aprili, submitted to *Physical Review B* (2014).